The Shell Structure of Matter Spaces

1. Introduction

The wave exchange of matter, space, rest, and motion (or more simply called matter-space-time) is in the nature of all physical phenomena. Therefore, the probability of possible states must have also the wave character and reflect the states of rest and motion. The possibility of rest and motion gives birth to the potential-kinetic field of reality, where rest (a potential field) and motion (a kinetic field) are inseparably linked between themselves in the unit potential-kinetic field.

This is why we describe the possibility of potential-kinetic wave processes by the corresponding wave probability of rest-motion. Thus, speaking about the *probabilistic wave field*, or the field of probability, we bear in mind an *ideal image of the wave of possibility and reality, including its nature*.

The wave theory of probability considers kinematics of wave probabilistic processes as the effect of wave interactions. It means that this theory is not interested in the consideration of fields of wave interactions – the contents of the processes; but it is interested only in their form, i.e., in the kinematic spatial geometry of wave processes.

2. Phase and energetic probabilities; the probability potential

Thus, the ***measure*** of the wave of possibility is the ***wave of probability*** under which we mean, by the definition, the ***mathematical image of the wave of possibility***. We will also call such probability the *phase probability* and denote it by the symbol $\hat{p}$.

We distinguish two opposite phase probabilities, the *kinetic* p_k and *potential* p_p, which express the probability of states of motion and rest.

The kinetic and potential phase probabilities define the *potential-kinetic phase probability*

$$\hat{p} = p_p + ip_k , \tag{1}$$

where i is the unit of negation (see the paper "The System of Primordial Concepts in Dialectical Physics (Outline)" and Introduction (http://www.bu.edu/wcp/Papers/Logi/LogiShpe.htm)).

The *density of phase probability* $\hat{\Psi}$ describes the distribution of phase probability $\hat{p}$:

$$\hat{\Psi} = \frac{d\hat{p}}{dV} = \frac{dp_p}{dV} + i\frac{dp_k}{dV} = \Psi_p + i\Psi_k , \tag{2}$$

where $d\hat{p}$ is the elementary phase probability, dV is the elementary volume of space, Ψ_p and Ψ_k are, correspondingly, the potential and kinetic densities of phase probability.

We further assume that the phase probability $\hat{p}$ (1) and its density $\hat{\Psi}$ (2) satisfy the *wave probabilistic equations*:

$$\Delta\hat{p} = \frac{1}{c^2}\frac{\partial^2\hat{p}}{\partial t^2}, \qquad \Delta\hat{\Psi} = \frac{1}{c^2}\frac{\partial^2\hat{\Psi}}{\partial t^2}. \tag{3}$$

The phase probability $\hat{p}$ and its *density* $\hat{\Psi}$ *must describe any wave events*. In every concrete case, the character of studying objects and the concrete chosen parameters-measures of the description are determined by these events.

If the density of energy of the field is proportional to the wave amplitude of density of phase probability squared, then

$$\frac{dE_p}{dV} = \zeta_p\Psi_p^2, \qquad \frac{dE_k}{dV} = \zeta_k\Psi_k^2, \qquad \frac{dE}{dV} = \zeta_p\Psi_p^2 + \zeta_k\Psi_k^2 , \tag{4}$$

where dE_p, dE_k, and dE are differentials of the potential, kinetic, and total energy; ζ_p and ζ_k are some coefficients of proportionality depending on the selection of phase probability and on the character of the field. For the class of fields satisfying the condition $\zeta_p = \zeta_k = \zeta$, we have

$$\frac{dE}{dV} = \zeta(\Psi_p^2 + \Psi_k^2) = \zeta\left|\hat{\Psi}\right|^2 . \tag{5}$$

Along with the phase probability, we operate with the notion of *energetic probability*. It is needed due to the simple reason that the distributions of total energy and masses are different (although they are related between themselves in the wave field-space of exchange). We must distinguish them.

The differential of energetic probability *dw*, by the definition, should be assumed to be proportional to the differential of energy *dE* , i.e.,

$$dw = \eta dE \,, \tag{6}$$

where η is the coefficient of proportionality.

In such a case the densities of potential, kinetic, and total *energetic probabilities* are determined as

$$\frac{dw_p}{dV} = \xi \Psi_p^2, \qquad \frac{dw_k}{dV} = \xi \Psi_k^2, \qquad \frac{dw}{dV} = \xi \left|\hat{\Psi}\right|^2, \tag{7}$$

where $\xi = \zeta\eta$ is the coefficient of proportionality depending on the character of the field and the choice of the wave function $\hat{\Psi}$.

The characteristic elements of the wave probabilistic geometry – extremes and zero of the functions Ψ_k and Ψ_p – define its discrete structure.

Potential and kinetic extremes are mutually conjugated because the conjugated functions

$$\hat{\Psi} = \Psi_p + i\Psi_k \quad \text{and} \quad \hat{\Psi} = i(\Psi_p + i\Psi_k) = (-\Psi_k)_p + i(\Psi_p)_k \tag{8}$$

satisfy the wave equation (3). Moreover, these extremes are also "conjugated" to zero of the wave function because the kinetic extremes spatially coincide with the potential zero and the potential extremes are spatially imposed upon the kinetic zero.

The extremes and zero of Ψ_k and Ψ_p functions coincide with the extremes and zero of their squares, Ψ_k^2 and Ψ_p^2, in three-dimensional space of reality. Therefore, they define the same probabilistic geometry of density of states and the energies related to the extremes and zero.

Since the wave functions $\hat{p}$ and $\hat{\Psi}$ satisfy the same wave equation (3), the extremes and zero of phase probability $\hat{p}$ and its density $\hat{\Psi}$ coincide. Hence, in this sense, the functions $\hat{p}$ and $\hat{\Psi}$ are equivalent.

The value of the constant coefficient (the normalizing factor) of the $\hat{\Psi}$-function does not matter because only its extremes and zeros define the discrete structure of a studying object. Therefore, it makes sense to introduce the notion the ***probabilistic potential*** (or the ***probability potential***) proportional to the wave function, which we also designate by the symbol $\hat{\Psi}$.

The wave *probabilistic potential* $\hat{\Psi}$ in the spherical polar coordinates (with the physical polar Z-axis) is represented in the form of the product of the four multiplicative components-functions of probability: $\hat{R}(\rho)$ (where $\rho = kr$), $\Theta(\theta)$, $\hat{\Phi}(\varphi)$, and $\hat{\Xi}(t)$, which represent by themselves the multiplicative components of probability potential.

The radial, polar and azimuth components of the potential of probability form the *spatial amplitude of the potential of probability* $\hat{\psi}(\rho,\theta,\varphi) = \hat{R}(\rho)\Theta(\theta)\hat{\Phi}(\varphi)$. Thus, the potential of probability $\hat{\Psi}$,

$$\hat{\Psi} = \hat{R}(\rho)\Theta(\theta)\hat{\Phi}(\varphi)\hat{\Xi}(t) = \hat{\psi}(\rho,\theta,\varphi)\hat{\Xi}(t) \,, \tag{9}$$

is determined by the product of spatial and time potentials of probability. Their amplitudes are described, in accordance with (3), by the following equations:

$$\Delta\hat{\psi} + k^2\hat{\psi} = 0 \,, \tag{10}$$

and

$$\frac{d^2\hat{\Xi}}{dt^2} = -\omega^2\hat{\Xi} \,. \tag{11}$$

After the conventional separation of variables, the wave equation (10) falls into the equations of radial $\hat{R}_l(\rho)$, polar $\Theta_{l,m}(\theta)$, and azimuth $\hat{\Phi}_m(\varphi)$ components:

$$\frac{d^2R_l}{d\rho^2} + \frac{2}{\rho}\frac{dR_l}{d\rho} + \left(1 - \frac{l(l+1)}{\rho^2}\right)R_l = 0 \,, \tag{12}$$

$$\frac{d^2\Theta_{l,m}}{d\theta^2} + ctg\,\vartheta\frac{d\Theta_{l,m}}{d\theta} + \left(l(l+1) - \frac{m^2}{\sin^2\theta}\right)\Theta_{l,m} = 0 \,, \qquad \frac{d^2\hat{\Phi}_m}{d\varphi^2} = -m^2\hat{\Phi}_m \tag{13}$$

Solutions and, in the definite degree, the form of the radial equation (12) depend on the concrete problem, which imposes the definite requirements on k^2. However, for any model of an object of study,

the *radial solutions define the* ***characteristic radial shells****, i.e. the shells of characteristic values of arguments of radial functions, which include both extremes and zeros of corresponding radial functions (potential and kinetic).* For a variety of problems, it is sufficient to know that such characteristic shells (spheres) exist. It is very important for determination of the spatial geometry of a studying object.

3. Radial shells of the wave spherical field of possibility and reality

Let us consider the structure of spherical objects of matter-space-time assuming that the wave vector *k* is constant. Under such approach (which represents the simplest solution), the *k*-vector is determined by the fundamental "carrier" frequency ω. At the atomic and subatomic levels, it is determined by the formula (5.15) (see the paper "*The System of Primordial Concepts in Dialectical Physics* (*Outline*)"). Therefore, radial functions are uniquely determined by the general structure of the equation (12).

At integer values of the wave number *m*, an elementary solution of the wave equation (10) has the standard form. If we will present the number *m* in the form $m = \frac{1}{2}2s$, where $s \in N$, we arrive at

$$\hat{\psi} = A_l \hat{R}_l(\rho)\Theta_{l,s}(\theta)e^{\pm is\varphi} = A_l\sqrt{\pi/2\rho}H^{\pm}_{l+1/2}(\rho)\Theta_{l,s}(\theta)e^{\pm is\varphi} \tag{14}$$

or

$$\hat{\psi} = A_l\sqrt{\pi/2\rho}(J_{l+1/2}(\rho) \pm iY_{l+1/2}(\rho))\Theta_{l,s}(\theta)e^{\pm is\varphi}, \tag{15}$$

where $\rho = kr$; $H^{\pm}_{l+1/2}(\rho)$, $J_{l+1/2}(\rho)$ and $Y_{l+1/2}(\rho)$ (or $N_{l+1/2}(\rho)$) are the *Hankel*, *Bessel* and *Neumann* functions, correspondingly; and A_l is the constant factor.

Solutions of the type (14), we call the even solutions.

It is convenient to present the radial component of the "amplitude" function in the following form

$$\hat{R}_l(\rho) = \frac{A\hat{e}_l(\rho)}{\rho} = A\frac{c_l(\rho) \pm is_l(\rho)}{\rho} = A(j_l(\rho) \pm iy_l(\rho)), \tag{16}$$

where

$$\hat{e}_l(\rho) = \sqrt{\frac{\pi\rho}{2}}H^{\pm}_{l+1/2}(\rho) = \rho h^{\pm}_l(\rho), \tag{17}$$

and *A* is the constant factor, determined on the basis of definite conditions.

If the radial component

$$A\frac{c_l(\rho)}{\rho} = Aj_l(\rho) \tag{18}$$

describes the potential radial field, then the component

$$A\frac{is_l(\rho)}{\rho} = Aiy_l(\rho), \tag{19}$$

describes the kinetic radial field. And vice versa, if the function (18) expresses the kinetic field then the equation (19) – the potential field.

Under the condition $\rho >> 1$, the Hankel function is determined by the approximate equality

$$H^{\pm}_{l+1/2}(\rho) \approx \sqrt{\frac{2}{\pi}}\frac{e^{i\left(\frac{l\pi}{2}+\frac{\pi}{2}\right)}}{\sqrt{\rho}}e^{\pm i\rho} = \sqrt{\frac{2}{\pi}}\frac{\hat{a}_l e^{\pm i\rho}}{\sqrt{\rho}}, \tag{20}$$

where

$$\hat{e}_l(\rho) = \sqrt{\frac{\pi\rho}{2}}H^{\pm}_{l+1/2}(\rho) \approx \hat{a}_l e^{\pm i\rho} \tag{21}$$

and

$$\hat{a}_l = e^{i\left(\frac{l\pi}{2}+\frac{\pi}{2}\right)}.$$

The function (21) can be called the spherical exponential, because at $\rho >> 1$ it is proportional to $e^{\pm i\rho}$. The functions $j_l(\rho)$, $y_l(\rho)$ (or $n_l(\rho)$), and $h^{\pm}_l(\rho)$, entering in (16) and (17), are Bessel's functions, correspondingly, of the first, second, third, and forth kinds.

The components of the spherical exponential

$$c_l(\rho) = \sqrt{\frac{\pi\rho}{2}} J_{l+1/2}(\rho) = \rho j_l(\rho) \tag{22}$$

and

$$s_l(\rho) = \sqrt{\frac{\pi\rho}{2}} N_{l+1/2}(\rho) = \rho y_l(\rho), \tag{23}$$

we call, correspondingly, the spherical cosine and sine.

Thus, at significant distances from the central domain of the spherical field, the radial function is represented by two harmonic spherical waves, one of which propagates from the center, another one converges on the center of the spherical field:

$$\hat{R}_l(\rho) \approx A\hat{a}_l e^{-i\rho}/\rho, \qquad \hat{R}_l(\rho) \approx A\hat{a}_l e^{+i\rho}/\rho. \tag{24}$$

The radial function (24) with the negative sign of its exponent defines the divergence wave, whereas the function with the positive sign of its exponent – the convergent wave. For this reason, signs ”–“ and “+” in the expression (16) define, correspondingly, the divergent and convergent radial waves.

We will supplement solutions of the equation (10) with the half-integer solutions at $l = m = (1/2)s$:

$$\hat{\psi} = A\hat{R}_s(\rho)\Theta_s(\theta)e^{\pm i\frac{s}{2}\varphi}, \tag{25}$$

where

$$\hat{R}_s(\rho) = \sqrt{\pi/2\rho}\, H^{\pm}_{\frac{s}{2}+\frac{1}{2}}(\rho), \tag{26}$$

$$\Theta_s(\theta)e^{\pm i\frac{s}{2}\varphi} = C_s \sin^{\frac{s}{2}}\theta(\cos\frac{s}{2}\varphi \pm i\sin\frac{s}{2}\varphi). \tag{27}$$

As follows from the equation (27), the polar extremes of odd solutions lie in the equatorial plane [1].

All spatial components are determined with the accuracy of a constant factor A, imposed by boundary conditions, which have no influence on the peculiarity of distribution of the nodes of radial spheres. The superposition of even and odd solutions defines the even-odd solutions. Odd solutions describe the nodes, lying in the equatorial plane of atomic space. In this plane, there are also rings of space separated by the radial unstable shells. A similar structure is widespread in the Universe. For example, big planets of the solar system have rings of matter on such shells. Potential and kinetic nodes specify the discrete geometry of the wave field-space.

Usually, in the simplest solutions of a series of classical problems, the Neumann function is not considered because of a simple reason: under $\rho \to 0$ it moves towards infinity. This is not admitted in the analysis of microobjects, since a radius of the minimal shell, $\rho_{\min} = kr_{\min}$, limits the minimal value of ρ-parameter.

Thus, the potential and kinetic spatial components of Ψ-potential have the following form

$$\hat{\psi}_p = Ac_l(\rho)/\rho = A\sqrt{\pi/2\rho}\, J_{l+1/2}(\rho)\Theta_{l,m}(\theta)e^{\pm im\varphi}, \tag{28}$$

$$\hat{\psi}_k = \pm As_l(\rho)/\rho = \pm A\sqrt{\pi/2\rho}\, N_{l+1/2}(\rho)\Theta_{l,m}(\theta)e^{\pm im\varphi}. \tag{28a}$$

4. The space distribution of extremes of the probabilistic potential; the periodic law of atomic structures

Two elementary polar-azimuth solutions of the equations (13) and (14) take the following form

$$Y_{l,m}(\theta,\varphi)_p = C_{l,m}C_m\Theta_{l,m}(\theta)\cos(m\varphi+\alpha), \quad Y_{l,m}(\theta,\varphi)_k = C_{l,m}C_m\Theta_{l,m}(\theta)\sin(m\varphi+\alpha). \tag{29}$$

where α is the initial phase of the azimuth state.

We term the first solution of (29) the *potential polar-azimuth component* of density of phase probability, and the second one – the *kinetic component*. Both solutions define the *potential-kinetic polar-azimuth component of density of phase probability*

$$Y_{l,m}(\theta,\varphi) = C_{l,m}C_m\Theta_{l,m}(\theta)\exp(i(m\varphi+\alpha). \tag{30}$$

The reduced polar-azimuth potential functions, $\widetilde{Y}_{l,m}(\theta,\varphi)=\widetilde{\Theta}_{l,m}(\theta)\cos m\varphi$, are presented in Table 1. (For reduced functions, the normalizing constant factors are equal to the numerical unit)

TABLE 1.

Reduced polar-azimuth potential functions $\widetilde{Y}_{l,m}(\theta,\varphi)$

l	m	$\widetilde{Y}_{l,m}(\theta,\varphi)=\widetilde{\Theta}_{l,m}(\theta)\cos m\varphi$			
0	0	1			
1	0	$\cos\theta$	5	0	$\cos\theta(\cos^4\theta - 10/9\cos^2\theta + 5/21)$
	±1	$\sin\theta\cos\varphi$		±1	$\sin\theta(\cos^4\theta - 2/3\cos^2\theta + 1/21)\cos\varphi$
2	0	$\cos^2\theta - 1/3$		±2	$\sin^2\theta\cos\theta(\cos^2\theta - 1/3)\cos 2\varphi$
	±1	$\sin\theta\cos\theta\cos\varphi$		±3	$\sin^3\theta(\cos^2\theta - 1/9)\cos 3\varphi$
	±2	$\sin^2\theta\cos 2\varphi$		±4	$\sin^4\theta\cos\theta\cos 4\varphi$
3	0	$\cos\theta(\cos^2\theta - 3/5)$		±5	$\sin^5\theta\cos 5\varphi$
	±1	$\sin\theta(\cos^2\theta - 1/5)\cos\varphi$			
	±2	$\sin^2\theta\cos\theta\cos 2\varphi$	6	0	$\cos^6\theta - 15/11\cos^4\theta + 5/11\cos^2\theta - 5/231$
	±3	$\sin^3\theta\cos 3\varphi$		±1	$\sin\theta\cos\theta(\cos^4\theta - 10/11\cos^2\theta + 5/33)\cos\varphi$
4	0	$\cos^4\theta - 6/7\cos^2\theta + 3/35$		±2	$\sin^2\theta(\cos^4\theta - 6/11\cos^2\theta + 1/33)\cos 2\varphi$
	±1	$\sin\theta\cos\theta(\cos^2\theta - 3/7)\cos\varphi$		±3	$\sin^3\theta\cos\theta(\cos^2\theta - 3/11)\cos 3\varphi$
	±2	$\sin^2\theta(\cos^2\theta - 1/7)\cos 2\varphi$		±4	$\sin^4\theta(\cos^2\theta - 1/11)\cos 4\varphi$
	±3	$\sin^3\theta\cos\theta\cos 3\varphi$		±5	$\sin^5\theta\cos\theta\cos 5\varphi$
	±4	$\sin^4\theta\cos 4\varphi$		±6	$\sin^6\theta\cos 6\varphi$

Polar components $\Theta_{l,m}(\theta)$ of space density of probability $\hat{\Psi}$ (Fig. 1a) define characteristic parallels of extremes and zeros (principal and collateral) on radial spheres (shells). Azimuth components $\Phi_m(\varphi)$ define characteristic meridians of extremes and zeros. Potential and kinetic polar-azimuth probabilities select together the distinctive coordinates (points) of extremes and zeros on the radial spheres (Fig. 1b-d). Graphs of these functions (Fig. 1 and Table 2) show that there are principal and collateral extremes, which determine, respectively, stable and metastable states of probabilistic events.

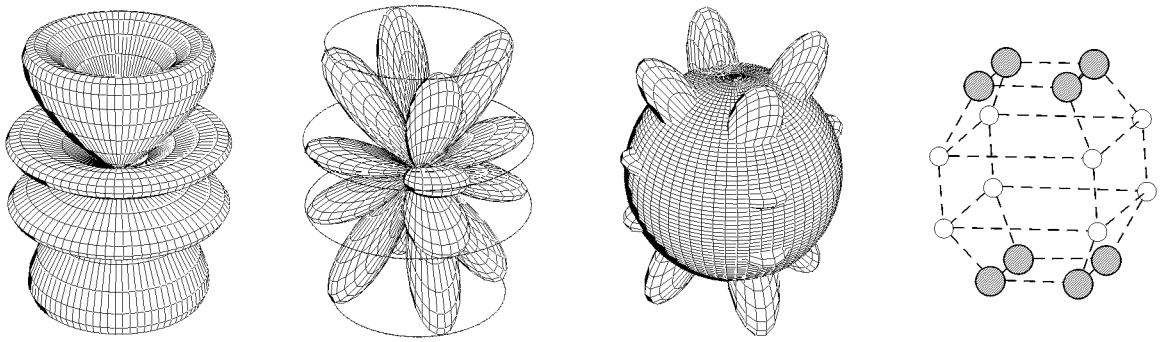

a) b) c) d)

Fig. 1. The graphs of the polar $\Theta_{5,2}(\theta)$ (a) and polar-azimuth $Y_{5,2}(\theta, \varphi)$ (b) functions; extremes of the function $Y_{5,2}(\theta, \varphi)$ on the characteristic radial shell $R_5(r)$ (c) distinguishing the disposition of extremes-nodes (d) (principal and collateral, black and white circles), in the spherical field of probability.

At m=0, the azimuth function $\Phi(\varphi)$ defines the Z-axis as the axis of phase probability of infinite-fold symmetry, at $m \neq 0$ Z-axis is the axis of 2m-fold symmetry. Twelve-fold symmetry (m=6) was found by S. Mae [2]. As follows from the equality (29), geometry of the potential polar-azimuth probability $Y_{l,m}(\theta,\varphi)_p$ will be the same as for the kinetic probability if the first one will be turned around the Z-axis at a right angle. In this sense, the geometries of spaces of rest and motion are mutually perpendicular.

The discrete geometry of polar, principal, and collateral extremes of the potential phase probability Ψ_p, shown in Table 2, gives the descriptive images of the phase wave probability. The black spheres indicate the vicinities of principal extremes. The white spheres of a smaller diameter show, conditionally, the collateral ones. Conditionally, all nucleon shells are drawn in Table 2 in a scale of radial spheres of the same radius.

TABLE 2. Solutions of the wave probabilistic equation $\Delta\hat{\Psi} = \frac{1}{c^2}\frac{\partial^2\hat{\Psi}}{\partial t^2}$ presented in the form of the space distribution of potential extremes-nodes (discrete elements of the shell nucleon structure of atoms); numbers 1, 2, 3, … , 110 are the ordinal numbers of the principal polar-azimuth nodes coinciding with the atomic numbers of elements *Z*.

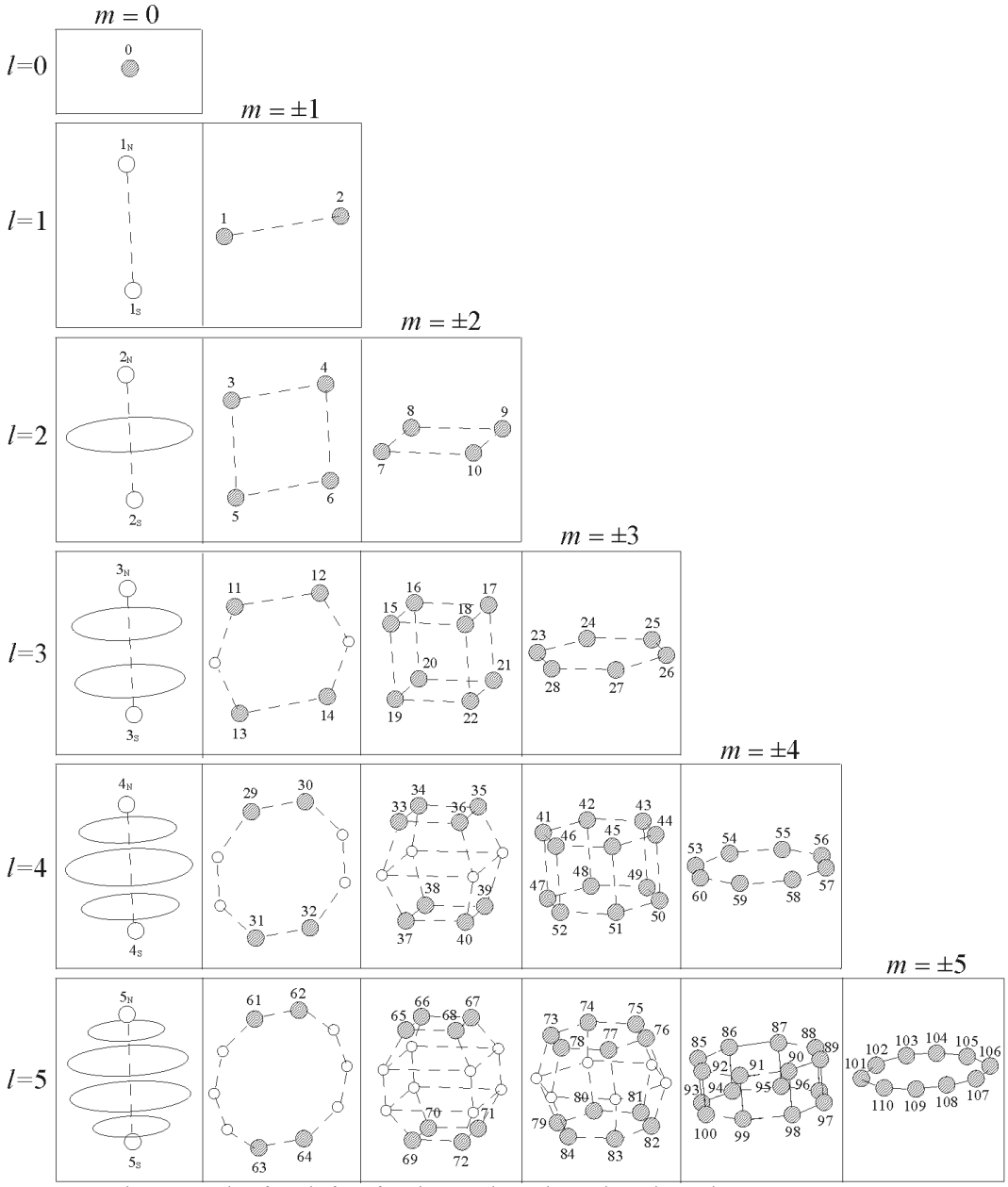

"N" and "S" are subscripts designating the "north" and "south" polar nodes (at $m = 0$).

In extremes, principal and collateral, the definite structural units of wave objects are localized. In Cosmos, approximately a half of all stars are double. Accordingly, we can assume that at the atomic level in extremes, at the most, two nucleons can also be disposed. The number of structural units, localized in an extreme, defines the multiplicity of its completing. We will call all extremes simply, the *nodes of shells*.

The two polar extremes, “north” and “south” (the white circles designated in Table 2 by the symbols l_N and l_S, where l=1, 2, 3...), and the circular extremes-meridians (beginning from l=2) characterize the radial shells at m=0; therefore, all these shells are almost similar.

Principal potential nodes (denoted in Table 2 by ordinal numbers) define the discrete geometry of probabilistic radial polar-azimuth wave shells at $m \neq 0$; they are determined by the functions:

$$\Psi_p = C_\Psi R_l(\rho)\Theta_{l,m}(\theta)\cos(m\varphi+\alpha), \qquad (31)$$

where $C_\Psi = C_{l,m}\Phi_m$ is the constant factor and $\rho = kr$ is the radius of characteristic shells, i.e., the shells with the zero or extremal value of radial functions.

For the kinetic nodes, we have

$$\Psi_k = C_\Psi R_l(\rho)\Theta_{l,m}(\theta)\sin(m\varphi+\alpha). \qquad (32)$$

As was mentioned above, there is the difference between distributions of two kinds of extremes: (1st) the density of phase probability $\hat{\Psi}$ and (2nd) the density of energy of wave fields proportional to $\left|\hat{\Psi}\right|^2$. This difference is demonstrated in Fig. 2.

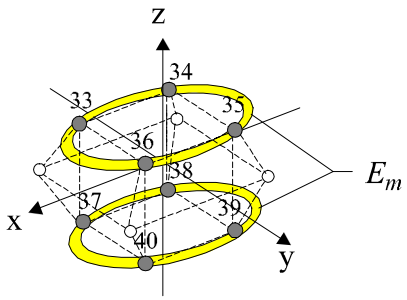

Fig. 2. Distribution of extremes of probabilistic states (small black and white spheres) and extremes of the total energy E_m (large toroidal circumferences) for the shell with l=4, m=±2.

To the definite extent, every principal node with the ordinal number Z bounds all previous shells with their nodes, which, as whole, require the definite designation. We denote such a bounded formation by the symbol ${}_ZX$. The subscript Z indicates the number of principal nodes and, simultaneously, the ordinal number of the last principal node of a probabilistic object. Thus, X is an arbitrary symbol of the wave object of shell structure. Having the specific spatial structure, every such object is distinguished from all others by the specific unrepeatable properties. A totality of discrete units (nodes) of the wave probabilistic field is considered as an element (“atom”) of such the abstract discrete-wave field.

The completely realized polar-azimuth n-th shell of the potential nodes of an abstract atom is defined, in accordance with the wave equation of probability (3), by the function

$$\Psi_{l,m}(\rho_{l,n},\theta,\varphi)_p = C_\Psi R_l(\rho_{l,n})\Theta_{l,m}(\theta)\cos(m\varphi+\alpha), \qquad (33)$$

where $\rho_{l,n}$ is the radius of n-th characteristic radial shell of the function $R_l(\rho)$. We will call such shells the *whole shells*. The geometry of shells is determined by the polar-azimuth functions. Graphs of some integer solutions of $\Theta_{l,m}(\theta)\cos(m\varphi+\alpha)$ and their sections are presented in Fig. 3.

The last shells of ${}_1H$, ${}_2He$, ${}_{10}Ne$, and ${}_{28}Ni$, presented on the right side in Fig. 3, are, correspondingly, the polar shells $\Theta_{1,0}(\theta)$, $\Theta_{2,0}(\theta)$, $\Theta_{3,0}(\theta)$, and $\Theta_{4,0}(\theta)$. They define the structure of some shorter-lived heavier isotopes of these elements. In the case of carbon atom, the difference between two images is in the form of the functions, $\Theta_{1,1}(\theta)\cos\varphi$ (the left picture) and $\Theta_{1,1}(\theta)\cos(\varphi+\pi/2)$ (the right picture).

The first form of carbon has a plane structure, the second one – an octahedral structure. The last apparently responses for the formation of the diamond like structure of carbon. In some degree, it is similar to the structure of external shells of silicon ${}_{14}Si$. Looking at these pictures, it is natural to come to the conclusion that polar nodes form, figuratively speaking, as if the “spinal” of atoms.

The partial realization of “*fractional*” *shells* is defined by the half-integer solutions [1] of the following kind

$$\Psi_{l,l}(\rho_{l,n},\theta,\varphi)_p = C_\Psi R_l(\rho_{l,n})\sin^l\theta\cos(l\varphi+\alpha) \qquad (34)$$

where l is a real number, with extremes lying in the equatorial plane.

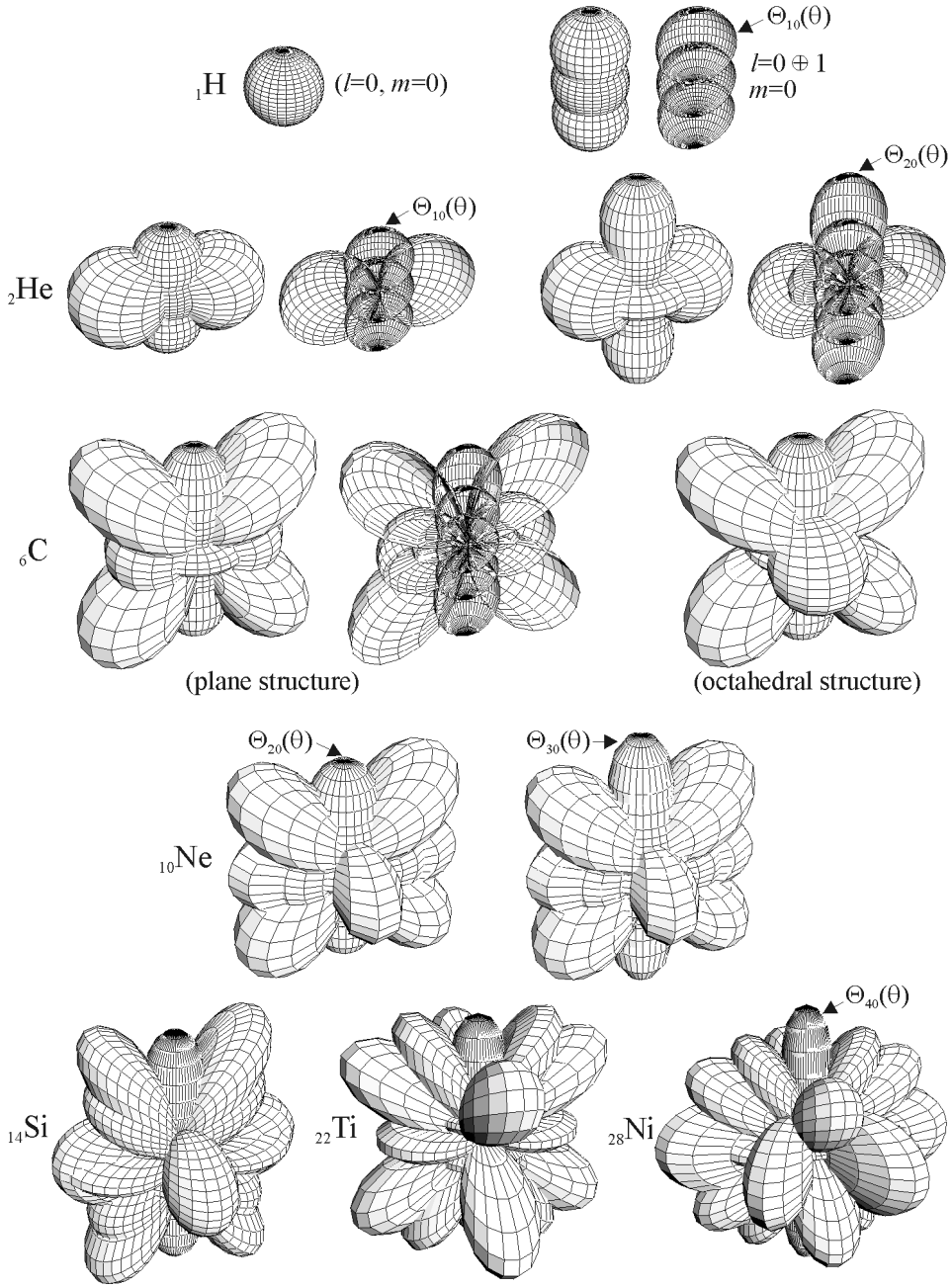

Fig.3. The structure of polar-azimuth whole shells for hydrogen $_1H$, helium $_2He$, carbon $_6C$, neon $_{10}Ne$, silicon $_{14}Si$, titanium $_{22}Ti$, and nickel $_{28}Ni$.

At $l = m = \frac{1}{2}s$, $s = 0, 1, 2, 3, \ldots$, we obtain the half-integer solutions

$$\Psi_s(\rho_{s,j},\theta,\varphi)_p = C_\Psi R_s(\rho_{s,j})\sin^{s/2}\theta\cos(s/2\,\varphi+\alpha), \qquad (34a)$$

where $\rho_{s,j}$ is the radius of the characteristic half-integer j-shell of the function $R_s(\rho)$.

For s = 1, only one-half of the azimuth wave is placed on the equator of an external shell. It defines one extremum and Z-axis of the first-fold symmetry. If s = 2, the function (34a) defines two extremes and the second-fold axial symmetry; s = 3 results in the three extremes and third-fold symmetry Z-axis, etc. Half-integer solutions in the equatorial domain have any-fold symmetry that attracts the special attention of modern researchers. In particular, the five-fold symmetry, strictly forbidden by the mathematical laws of crystallography, was observed in 1984 [3].

Half-integer solutions at s = 1 describe the azimuth wave of probability in the equatorial plane, which twice rotates the equator. In such a traveling wave during a half-period, signs of parameters are changed into opposite.

Running twice the equator, the wave of probability repeats again. Hence, we can write

$$Y(\theta,\frac{s}{2}\varphi)=Y(\theta,\frac{s}{2}(\varphi+4\pi)), \qquad (35)$$

where $s=1, 2, 3, \ldots$, which takes place actually.

The common requirement of periodicity, $Y(\theta,\varphi)=Y(\theta,\varphi+2\pi)$, must mean that the one complete wave of probability is placed on the equator, but it is not in agreement with the aforementioned solutions.

In the general case, the complete structure of any element (abstract atom) is defined by the two sums

as $$\Psi_Z=\sum C_\psi R_l(\rho_{l,n})\Theta_{l,m}(\theta)\cos(m\varphi+\alpha_m)\oplus\sum C_s R_s(\rho_{s,j})\sin^{s/2}\theta\cos\left(\frac{s}{2}\varphi+\beta_s\right). \qquad (36)$$

Thus, the first sum in (36) consists of embedded whole shells, the second sum consists of embedded half-integer subshells.

The initial phases, α_m and β_s, characterize a mutual azimuth orientation of polar-azimuth shells and subshells of the atomic space with respect to the polar Z-axis. They are expressed by the vector of initial phases $\alpha=(\alpha_1,\ldots,\alpha_m;\beta_1,\ldots,\beta_s)$.

The polar shells (m = 0) are always the whole ones. They have axes of the infinite-fold symmetry and, hence, their mutual azimuth orientation does not matter.

The mutual azimuth orientation of polar-azimuth shells and subshells defines the space isomers of atoms.

The total number of nodes in an abstract atom, as a totality of probabilistic discrete units, its nodal measure, is easily defined from Table 2. The number of nodes, actually completed by matter (*H*-atoms, nucleons), and their multiplicity define the relative mass of the abstract atom.

According to the Table 2, the definite similarity of the geometry of external shells of abstract atoms takes place. Arranging the atoms with the same or similar structure of outer shells one under another, in accordance with Table 2, we arrive at the ***periodic-nonperiodic law of spherical spaces***.

If we take the symbols of the real elements of Mendeleev's periodic table in the capacity of symbols of probabilistic objects (atoms) originated from Table 2 (so that their ordinal numbers Z will coincide with the atomic numbers of real atoms), we arrive at Table 3.

We can speak now about a subsequent series of probabilistic elements as "atoms" of the discrete-wave field. Thus, Table 3 doubles Table 2 in the form of the traditional classification of chemical elements in the order of their atomic numbers. In the light of the above-mentioned, Table 3 can be regarded as the *generalized quasiperiodic law of atomic structure of matter-space-time and possibility-reality*, or as the ***generalized table of elements***. We conditionally designated the last 110th element of the 5th period (l=5, m=5) in Table 3 as $_{110}$Ch (***chernobylium***).

TABLE 3. Solutions of the wave probabilistic equation $\Delta\hat{\Psi}=\frac{1}{c^2}\frac{\partial^2\hat{\Psi}}{\partial t^2}$ presented in the traditional form of the periodic law of chemical elements; or the quasiperiodicity as a result of similarity of the structure of external shells of abstract atoms drawn in Table 2.

5. *The structure of carbon atom in the light of new solutions and probabilistic elements-isotopes*

Thus, elementary atomic objects of matter-space-time have the quasispherical structure, which is described by the wave equation in the spherical polar system of coordinates. As follows from the general solutions [4-6], elementary quasispherical atoms of matter-space-time and possibility-reality represent by themselves the system of characteristic shells with nodal points, expressing the discrete geometry of these shells. The number of polar-azimuth nodes Z expresses the ordinal number of the concrete atomic structure.

In the atomic model, in question, *H*-atoms as the main structural units of any atom are located in its potential nodes. The *H*-structure of atoms with *He*-components becomes apparent during the rebuilding of

atoms, accompanied with the emission of *He*-components (α-particles). The *H*-structure of atoms shows itself in different chemical (qualitative) reactions, etc.

A node of space is characterized by the *node multiplicity* η equal to the number of *H*-atoms in the node. For atoms of space and matter, η is equal to zero, one or two:

A successive series of solutions of the wave equation of matter-space-time is naturally determined by *ordinal numbers of principal azimuth nodes*, which are a natural bound of each elementary solution. These solutions are realized in objective space in the form of atoms of matter-space.

Ordinal numbers of principal azimuth nodes, we term *ordinal numbers of atoms of space* and *matter*.

The *relative mass of atoms*, defined in such a way, is equal to the total number of *H*-atoms located at shells of a concrete atom:

$$A = \sum_k Z_{pk}\eta_{pk} + \sum_i (Z_{gi}\eta_{gi} + Z_{vi}\eta_{vi}), \qquad (37)$$

where k and i are numbers of polar and azimuth shells, respectively;
Z_{pk} is the number of polar nodes of k-th polar shell;
Z_{gi} and Z_{vi} are the number of principal and collateral azimuth nodes, respectively, of i-th azimuth shell; η_{pk}, η_{gi} and η_{vi} are numbers of multiplicity of the corresponding nodes.

According to the above definition, the ordinal number of an atom is

$$Z = \sum_i Z_{gi} \ . \qquad (38)$$

Collateral extremes define the metastable states. Accordingly, the same probabilistic element ${}_ZX$ can be realized in real space with different relative masses. Besides, the relative mass depends on the real filling of polar nodes with *H*-atoms (nucleons). Hence, the same atom of the probabilistic field is represented by a series of its own "isotopes". The relative masses A of the probabilistic isotopes ${}^M_Z X$ are expressed by the formula (37).

Let us estimate an average relative mass of the abstract probabilistic element ${}_{72}Hf$. According to Table 2 and the formula (36), one of the minimal realizations of this element is characterized by the relative mass $({}_{72}Hf)_{\min} = 0\cdot 11 + 2\cdot 72 + 0\cdot 24 = 144$. The maximal structure with all completely filled nodes has the relative mass $({}_{72}Hf)_{\max} = 2\cdot 11 + 2\cdot 72 + 2\cdot 24 = 214$. Thus, the average mass of the abstract element ${}_{72}Hf$ is $\langle {}_{72}Hf \rangle = \dfrac{({}_{72}Hf)_{\min} + ({}_{72}Hf)_{\max}}{2} = 179$, whereas the mass number of real ${}_{72}Hf$ is 178.49.

A similar correspondence of mass numbers of abstract atoms (and their isotopes) of the probabilistic wave field and atoms (isotopes) of the real physical space undoubtedly cannot be regarded as a case and therefore requires further research within this area.

In the qualitative spectrum of elements (see Table 2), a particular place takes carbon (Z = 6), an element with nodes disposed in one plane. Its outer fully completed shell corresponds to the wave numbers $l = 2$ and $m = \pm 1$. Carbon is the basis of organic structures. The discrete geometry of shells of carbon, as an atom of bases of life, reminds us, in form, the Russian letter "Ж". In the Old Slavonic alphabet, this letter symbolizes life (in Russian, the word "жизнь" means life). The axis of symmetry of the carbon atom contains 5 polar nodes at $m = 0$ and $l = 0, 1, 2$.

The nodal structure of carbon atom ${}^{12}_6C$ and its polar-azimuth functions are as shown in Fig. 4. The symbolic designation of carbon (Fig. 4c) reflects the definite geometry of disposition of its six principal nodes and shows the shortest distances of exchange (interaction) between them.

The nodal-shell model obtained can account for the structure of different isotopes. By virtue of this, the last heavy and light unstable isotopes (that could be obtained in capture reactions at the neutron exposure on accelerators) of any element of the periodic table can be predicted theoretically. In particular, as we can see from Table 2 (which presents results of theoretical solutions), for carbon these are, respectively, *C*-22 and *C*-8 (see Fig. 5). Actually, it follows from the experimental data [7], naturally occurring carbon isotopes are *C*-12 (98.89%) and *C*-13 (1.11%), and unstable isotopes are *C*-8, *C*-9, *C*-10, *C*-11, *C*-14, *C*-15, *C*-16, *C*-17, *C*-18, *C*-19, *C*-20, *C*-21, and *C*-22.

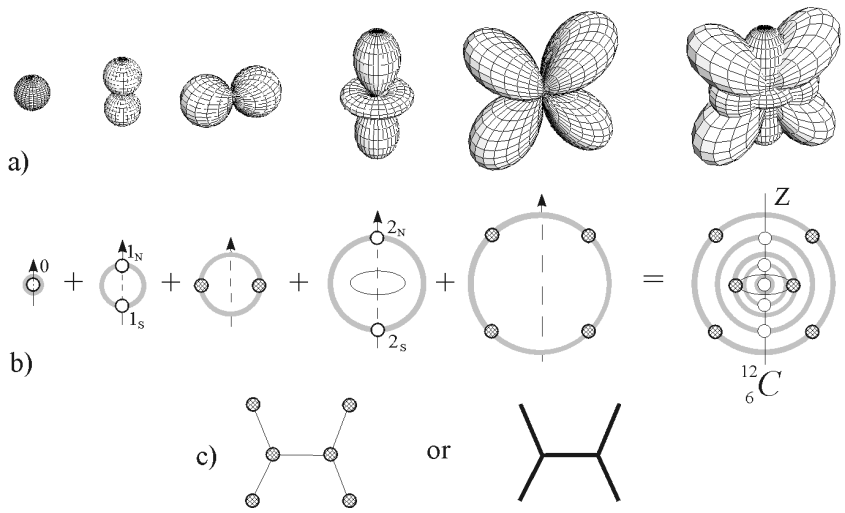

Fig. 4. Plots of polar-azimuth functions (a), their extremal points on radial extremal shells (b), and the symbolic designation of carbon ${}_6C$ (c).

Fig. 5. The possible isotopes of carbon.

For helium, the last heavy and light unstable isotopes are, respectively, *He*-14 and *He*-2 (Fig. 6); for neon – *Ne*-34 and *Ne*-16; for titanium – *Ti*-62 and *Ti*-36, for nickel – *Ni*-78 and *Ni*-50 [7], for neodymium – *Nd*-162 and *Ne*-108. For the most abundant element in the entire Universe, hydrogen, these are *H*-6 and *H*-1 (see Fig. 7); the experimental data confirm this [7]; etc. The difference between the shell structure of $^{3}_{1}H$ and $^{3}_{2}He$, $^{4}_{1}H$ and $^{4}_{2}He$, etc. is revealed as well on the basis of the probabilistic atomic model described.

Fig. 6. The possible isotopes of helium.

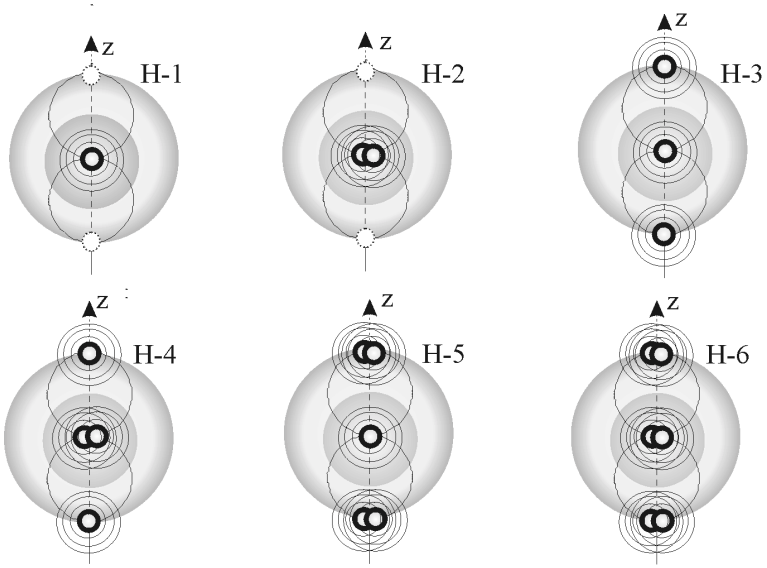

Fig. 7. The possible isotopes of hydrogen.

Individual properties, characteristic for every element (isotope) with the same ordinal number Z, are kept even when the principal azimuth nodes of external shells contain one nucleon in every node (as takes place, e.g., with $^{8}_{6}C$, see Fig. 5, and with $^{2}_{2}He$, Fig. 6). This happens because the geometry of external polar-azimuth shells is not changed in this case (of course, during the lifetime of the isotope). Thus, the difference between the structure of different isotopes is defined only by the multiplicity of completing of all nodes, including polar ones, within the shells, characteristic for a definite atom. The characteristic shells of the carbon atom are presented in Fig. 4.

The structure of nucleon shells of atoms is responsible for the geometry of molecules of the *linear*, *plane*, and *volumetric* forms.

The carbon atom *C* has the plane structure of disposition of all its nodes. A surrounding space, embracing the carbon, has a spherical shell in the equatorial domain with four vacant azimuth potential nodes (light dashed circles in Fig. 8). What the shell is it?

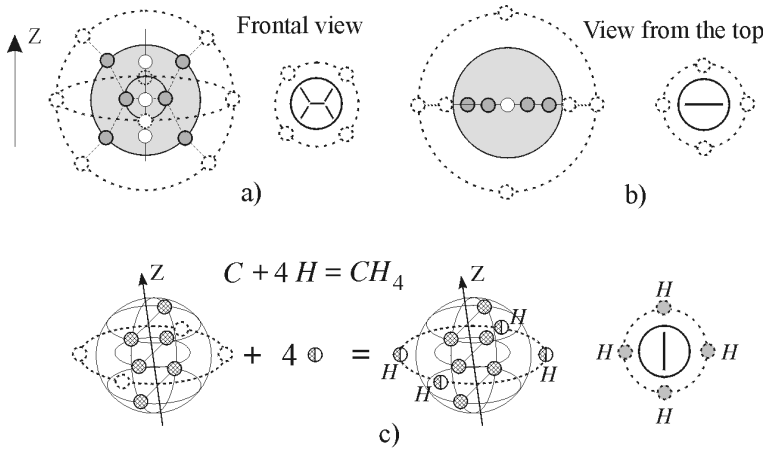

Fig. 8. The carbon structure (a, b) with the near empty spherical shells and nodes designated by dash lines; the formation of a methane molecule (c); the conditional designations of the structures are drawn on the right.

In hydrocarbon molecules, carbon represents basis. It has the external *n*-shell (l=2, $m = \pm 1$) with four potential-kinetic nodes entirely completed with nucleons (*H*-atoms). Outside this shell, the space of a shell with four empty nodes (l=2, $m = \pm 2$) follows (see Table 2). It belongs to the subsequent elements of the periodic table: ${}_7N$, ${}_8O$, ${}_9F$, and ${}_{10}Ne$. But this shell, in a certain sense, is, simultaneously, the free (empty) shell of carbon where four *H*-units can be localized as well. Such a shell can be called the ***improper*** shell of carbon.

When an improper shell is drawn into a process, a new atom does not form. A molecule with the structure, repeating the discrete geometry of corresponding atoms of the given shell, is formed. In a case with a methane molecule CH_4 (Fig. 8), its analog is neon. Under definite conditions, nodes of the improper shell can be completed with *H*-atoms. As a result, a methane molecule CH_4 is formed (Fig. 8c).

Moreover, for fixed l and m, the whole class exists of geometrically similar shells of the l-th radial function [6]. In Fig. 8, a dash circumference depicts such a shell (in the plane of disposition of all carbon nodes), repeating the outer shell of carbon with four nodes.

Some other possible structures of hydrocarbons (among innumerable ones), with participation of both aforementioned shells, are drawn in Fig. 9.

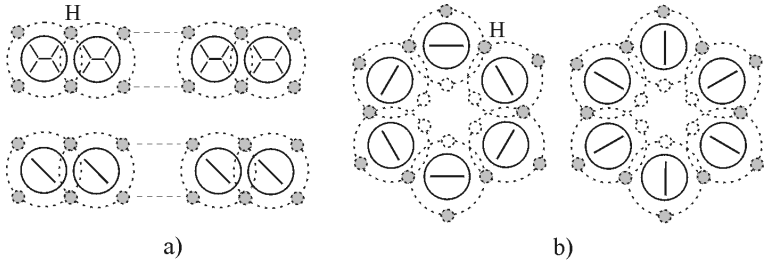

Fig. 9. The two possible structures of hydrocarbon molecules, $C_nH_{2(n+1)}$ (a) and cyclohexane C_6H_{12} (b) .

Herein, the distant binding energy, per one mole of substance, defining the characteristic energy of the break of such (chemical) bonds, is defined by the expression [6]:

$$E_e = \frac{e^2}{8\pi\varepsilon_0 \lambda\!\!\!^{-}_e} N_A = 433.1211762\ kJ/mol = 103.4492\ kkal/mol\,, \qquad (39)$$

where $\lambda\!\!\!^{-}_e$ is the fundamental wave radius and $\varepsilon_0 = 1\ g/cm^3$ is the unit mass density.

Actually, upon tearing off the *H*-atom from a *n*-node of these (improper) shells, a definite energy is spent. According to the experimental data [8], this energy is equal to 101 *kkal/mol* for CH_4 and 104 *kkal/mol* for C_2H_4.

6. *Applications of the theory to crystals*

Because the theory of phase wave probability has the general discrete-wave feature; therefore, it can be applicable to an analysis of any discrete-wave material spaces, including also material spaces in the solid phase. Such physical spaces exist naturally in numerous minerals. Elementary characteristic directions of the probabilistic formation of space are determined by the polar-azimuth functions $Y_{l,m}(\theta,\varphi)_p = C_{l,m}C_m\Theta_{l,m}(\theta)\cos m\varphi$, it is natural to expect that the characteristic angles of this function are materialized in characteristic angles of the crystal forms of minerals.

Let us verify this supposition by comparing our calculations with experimental data compiled mainly by R. Haüy [9] and N. Kokscharov [10]. We will compare the characteristic angles of minerals, uninteresting in their composition, with the corresponding angles of the *reduced* (~) polar function of probability $\widetilde{\Theta}_{l,m}(\theta)$. Within this comparison, the sign "?" indicates a supposed correspondence.

We will denote zeros of functions $\widetilde{\Theta}_{l,m}(\theta)$ by the symbol $O_s(l,m)$, where *s* is the number of the corresponding root. Analogously, angles of extreme values $\widetilde{\Theta}_{l,m}(\theta)$ will be denoted as $\theta_s(l,m)$. The angles of zeros and extremes, their sums and differences, are characteristic angles of distribution of the phase density. Obviously, every angle is characterized simultaneously by two measures: θ and $\pi-\theta$. Only a small part of results of this comparison is presented in Table 4 (these supplement those presented in Table 3.1 of the work [5], pp. 232-253).

Table 4. Characteristic angles $\widetilde{\Theta}_{l,m}(\theta)$ and experimental values of the angles in crystal minerals.

Let us consider now the geometry of crystals from the point of view of typical angles of polar functions resting upon Haüy's works [9].

a). The pomegranate with 24 facets [9: p.82; 2*]. The scanning is 24 rhombuses. The angles of the rhombuses (Fig. 10a) are correspondingly equal [9: p.79; 1*]:

$\angle bac = 70^\circ 31' 44''$ → $O_2(5,3) = O_2(2,0) - O_1(2,0) = 70^\circ 31' 43.''60$,

$\angle acd = 109^\circ 28' 16''$ → $O_3(5,3) = 2O_1(2,0) = 109^\circ 28' 16.''40$

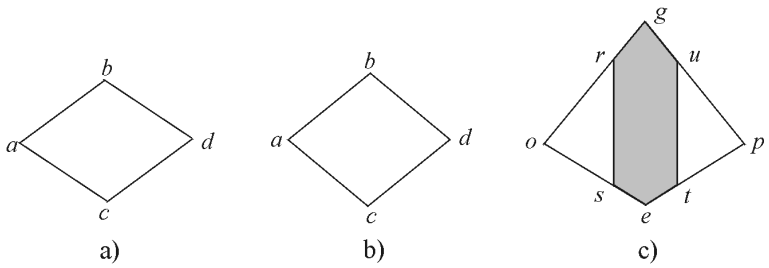

Fig. 10. Rhombic facets of some crystals.

b). The lime spar [9: p.36, 7*]. The scanning is 6 rhombuses (Fig. 10b) with angles:

$\angle bac = 78^\circ 27' 47''$ → $2O_1(3,0) = 78^\circ 27' 46.''94$,

$\angle acd = 101^\circ 32' 13''$ → $O_3(3,0) - O_1(3,0) = 2(O_3(3,0) - O_2(3,0)) = 101^\circ 32' 13.''06$

c). The pomegranate with 36 facets. The scanning is 12 rhombuses (Fig. 10a) and 24 prolate hexagonals ("*srgute*", Fig. 10c) [9: p.82; 2*].

$\angle rgu = 78^\circ 27' 47''$ → $2O_1(3,0) = 78^\circ 27' 46.''94$,

$\angle set = 117^\circ 02' 8''$ → $2O_2(6,3) = 117^\circ 02' 8.''50$,

$\angle gut = \angle grs = 140^\circ 46' 07''$ → $O_3(3,0) = 140^\circ 46' 06.''53$

$\angle rse = \angle etu = 121^\circ 28' 56''$ → $O_4(6,3) = 121^\circ 28' 55.''75$

$\angle goe = \angle gpe = 82^\circ 15' 03''$ → $180^\circ - (O_1(3,0) + O_2(6,3)) = 82^\circ 15' 02.''28$

7. *Final conclusion*

The *physical* structure of atoms can be understood only in the framework of a *physical* theory. Unfortunately, the modern quantum theory, which pretends to the complete description of atoms, is a *mathematical* theory. Accordingly, the quantum mechanical (Schrödinger's) atomic model does not reveal the *internal spatial* structure of atoms [5, 14] and, therefore, is a weak theoretical basis for applied sciences, in particular, for structural researches and nanotechnology.

Every sane physicist sees this, but not each assumes that the quantum mechanical atomic model, originated from the Rutherford-Bohr atomic (nuclear) model and perceived at present as a dogma, can be substituted with a physical atomic model, reflecting (simulating) reality at the atomic and subatomic levels. Such a fully formed view exists due to the domination of quantum mechanics. Therefore, although nanotechnology cannot continually develop successfully enough, actually blindly, without clarifying the real physical (spatial, volumetric) structure of individual atoms, this subject is not an objective of modern theoretical physics.

Mendeleev discovered the periodic system in 1869 as an *experimental* regularity. Since then, the nature of such a regularity (more concretely quasiperiodicity) inherent in chemical elements is a greatest mystery for physicists and chemists [15]. More than 700 variants of the *experimental* periodic system were proposed during 100 years after its discovery [16]. This status qua in natural science still exists in spite of "explanation" by quantum mechanics of the *electron shell structure* of atoms. The fact is that the *theoretical* variant of the periodic table of chemical elements is absent in modern physics and is still the problem for it.

The understanding of the quasiperiodicity is closely related with understanding of primordial fundamentals of natural science. The structure of atoms relates to them. We mean the *intratomic spatial* (*volumetric*) *geometry of disposition* of nucleons, being the main constituents of atoms. This geometry directly *relates to the symmetry*, inherent in material spaces *at all levels* of the Universe including atomic and subatomic, without any exception.

The quantum mechanical atomic model keeps the principal feature of the classical atomic model: it deals with the *nuclear* atomic model and the *main role attributes to electrons* (*electrons' energy structure* and *density*), i.e., the particles of the second order in comparison with nucleons. Herein, nuclear physics, using some tenths of different theoretical nuclear models, considers also only the *energetic structure* of nuclei. The lasts are regarded as the most massive part of atoms, extraordinarily minute in volume and tremendous in dense. The nucleus radius has been accepted to be related to the mass number A of an atom by the formula $1.2 \cdot 10^{-13} A^{1/3}$ *cm*. Accordingly, a nucleus is usually regarded as a mathematical point in comparison with an atom, whose radius is about 10^{-8} *cm*.

In this paper we presented the conceptually new approach to the problem of atomic structure, which rests on ideology of dialectical binary numbers [4, 17]. Publications of others, related to the approach accepted by the authors, are absent in literature. Relying on this approach, we described here in outline the derivation of the *internal spatial structure of atoms*, *morphology* of crystals, and the *theoretical periodic law* of atomic structures, where the *prevalent role* (in formation of these structures) *belongs to nucleons* [4-6, 14].

The simplest solutions of the wave equation (3) for the *spherical* wave field of space led to the discovery of the spatial structure of atoms. As it turned out, atoms are similar, in form, to Prout's quasispherical *H*-molecules [18]. The similarity of the structure of external atomic shells in turn led to the quasiperiodic series of real atoms of Mendeleev's table, revealing the nature of the periodic law. Accordingly, one can firmly state that properties of individual atoms (elements) are, mainly, defined by the nodal structure of their external shells.

The strict correspondence of mass numbers of obtained abstract atoms (and their isotopes), belonging to the *probabilistic* wave field, and the atoms (isotopes) of the *real* physical space undoubtedly cannot be regarded as a case and, therefore, requires further research within this area. Moreover, such a

correspondence points to the necessity to identify the mass of the nodal nucleon with the mass of *H*-atom. Atomic shells consisting of abstract structural units should be regarded then as the shells containing in their nodes *H*-atoms.

The physical (spatial) structure of carbon and all its isotopes, which were found experimentally [7], make clear as a result and presented here as an important example, especially for nanotechnology. Apparently, we are on the right way to understanding of the "*genetic code*" of the structural variety in nature, where fullerenes and carbon nanotubes are particular cases of its manifestation.

On the whole, all data concisely presented above and the other ones, obtained by the authors [4-6, 14], testify in favor of the *wave nature* of material spaces, including both microspaces of individual atoms (and their compounds) and megaspaces [19]. In particular, the interconnection and interdependency of different levels of the Universe prove themselves: at the macrolevel, in characteristic angles of crystals (Table 4), and at the microlevel, in the same in magnitude characteristic angles of disposition of nucleon nodes in atoms (Table 2). The spectrum of these angles defines the shape of crystals, i.e., morphology [20] and symmetry [21] of material spaces. Because of this, we can conclude too that the wave probabilistic equation (3) contains information about symmetry in nature.

Thus, there are potentially enormous benefits in prospect, in particular, for nanotechnology, from the further research within this area devoted, in essence, to the revelation of the *genetic code* of nature at the atomic and subatomic levels.

References

1. Magnus W. und Oberhettinger F., *Formeln und Sätze für die speziellen Funktionen der mathematischen Physik*, Spiengler-Verlag, Berlin-Heidelberg, 85, 1948.
2. Shinji Mae, *Tyndall Figures at Grain Boundaries of Pure Ice*, Nature, 257, No.5525, 1975, pp.382-383.
3. D. Shechtman, I. Blech, D. Gratias, and J.W. Chan, *Metallic Phase with Long-Range Orientation Order and no Translation Symmetry*, Phys. Rev. Lett., 53, No.20, 1984, pp.1951-1953.
4. L.G. Kreidik and G.P. Shpenkov, *Alternative Picture of the World*, Vols. 1 – 3, Bydgoszcz, 1996.
5. L.G. Kreidik and G.P. Shpenkov, *Foundations of Physics*; 13.644…*Collected Papers*, Bydgoszcz, 1998.
6. L.G. Kreidik, G.P. Shpenkov, *Atomic Structure of Matter-Space*, Bydgoszcz, 2001.
7. G. Audi and A.H. Wapsta, *The 1995 update to the atomic mass evaluation*, Nuclear Physics A595, Vol. 4, p. 409-480, December 25, 1995.
8. V.I. Vedeneev, et al., *The Chemical Bond Brake Energy* (in Russian), Moscow, 1962; A.P. Babichev, et al., *Physical Quantities*, Reference Book, Atomenergoizdat, Moscow, 1991.
9. Rene-Just Haüy, *La structure des cristaux*, Oeuvres choisies, (Russian translation), Izd. Akad. Nauk SSSR, 1962.
   1* *Sur la double refraction de plusieurs substances minerales*. Ann. De Chimie, 1793, XVII, pp.140-155, et Mém. De la Soc. d'Hist.nat. de Paris, an VII, pp.25-27.
   2* *Mémoire sur les méthodes mineralogiques*. Ann. Des Mines, 1793,XVIII, pp.225-240.
   3* *Description de la gemme orientale*. Bull. De la Soc. Philom., 1791, pp.49-50.
10. N. Kokscharov, Mining Journal, SPB, 1844-1878.
11. Goldschmidt V. *Atlas der Kristallformen*. Heidelberg, Bd.1-9, 1913-1923.
12. S. Glinka, Mining Journal, SPB, v. IV, N.10, 1889.
13. G. Lebedev, Mining Journal, SPB, v. I, N.2, 1875.
14. L.G. Kreidik, G.P. Shpenkov, *Important Results of Analyzing Foundations of Quantum Mechanics*, Galilean Electrodynamics, No , 2001, to be published.
15. Kazuo Saiti (Ed.), *Chemistry and Periodic Table*, Iwanami Modern Chemistry Series, No 5, Iwanami Shoten, Publ., 1979.
16. E.G. Mazur, *Graphic Representations of the Periodic System During One Hundred Years*, The University of Alabama Press, University, Al., 1974.
17. L.G. Kreidik, G.P. Shpenkov, *The Material-Ideal Numerical Field*, Proceeding of the Conference "CONTACT'95", Sofia, 1995, pp. 34-39.

18. W. Prout, *On the Relation of Specific Weights of Bodies in their Gaseous State to Weights of their Atoms*, Progress of Chemistry, 1940, V. 2-3, p. 288; Ann Phil., **VII**, 111-113, 1816.
19. L.G. Kreidik, G.P. Shpenkov, *Roots of Bessel Functions Define Spectral Terms of Micro- and Megaobjects*, Abstracts of the XIII *International Congress on Mathematical Physics*, 15 – 22 July 2000, London, UK, p.118.
20. L.G. Kreidik, G.P. Shpenkov, *A Wave Field of Probability and the Form of Crystals*, Abstracts of the XVIIIth IUCr (*International Union of Crystallography*) *Congress* & *General Assembly*, 4 – 13 August 1999, Glasgow, Scotland, UK, p. 258.
21. I. Hargittagi (Ed.), *Symmetry, Unifying Human Understanding*, Pergamon Press, New York, Oxford, 1986.